

Roberge-Weiss phase transition and its endpoint

Hiroaki Kouno,^{1,*} Yuji Sakai,^{2,†} Kouji Kashiwa,^{2,‡} and Masanobu Yahiro^{2,§}

¹*Department of Physics, Saga University, Saga 840-8502, Japan*

²*Department of Physics, Graduate School of Sciences,
Kyushu University, Fukuoka 812-8581, Japan*

(Dated: October 26, 2018)

Abstract

The Roberge-Weiss (RW) phase transition in the imaginary chemical potential region is analyzed by the Polyakov-loop extended Nambu–Jona-Lasinio (PNJL) model. In the RW phase transition, the charge-conjugation symmetry is spontaneously broken, while the extended \mathbb{Z}_3 symmetry (the RW periodicity) is preserved. The RW transition is of second order at the endpoint. At the zero chemical potential, a crossover deconfinement transition appears as a remnant of the second-order RW phase transition at the endpoint, while the charge-conjugation symmetry is always preserved.

PACS numbers: 11.30.Rd, 12.40.-y

*kounoh@cc.saga-u.ac.jp

†sakai@phys.kyushu-u.ac.jp

‡kashiwa@phys.kyushu-u.ac.jp

§yahiro@phys.kyushu-u.ac.jp

I. INTRODUCTION

One of the most fascinating and essential subjects in hadron physics is to explore the phase diagram of quantum chromodynamics (QCD). QCD is a remarkable theory in the sense that it is renormalizable and parameter free. The thermodynamics of QCD is well defined, nevertheless not clearly understood because of the nonperturbative nature. A powerful method of exploring the phase diagram is lattice QCD (LQCD) as the first-principle calculation, but it has the well known sign problem when the quark chemical potential (μ) is real; for example, see Ref. [1] and references therein. Although several approaches such as the reweighting method [2], the Taylor expansion method [3] and the analytic continuation to the real chemical potential (μ_R) from the imaginary chemical potential (μ_I) [4–11] have been proposed, these are still far from perfection.

So far the phase diagram in the μ_R region has been analyzed by effective models such as the Nambu–Jona-Lasinio (NJL) model [12–20] and the Polyakov-loop extended Nambu–Jona-Lasinio (PNJL) model [21–41]. The NJL model describes the chiral symmetry breaking, but not the confinement mechanism. The PNJL model is designed [23] to make it possible to treat both the mechanisms. It is reported that the confinement mechanism shifts the critical endpoint of the chiral phase transition toward larger T and smaller μ_R [29, 35, 37].

When the chemical potential is imaginary, that is $\mu = i\mu_I = iT\theta$, LQCD has no sign problem, so that LQCD data are available there [4–11]. The first essential work on the μ_I region was made by Roberge and Weiss (RW) [42]. They found that the thermodynamic potential $\Omega_{\text{QCD}}(\theta)$ has a periodicity, $\Omega_{\text{QCD}}(\theta) = \Omega_{\text{QCD}}(\theta + 2\pi k/3)$, for any integer k . The RW periodicity was proven by showing that $\Omega_{\text{QCD}}(\theta + 2\pi k/3)$ is reduced to $\Omega_{\text{QCD}}(\theta)$ with the \mathbb{Z}_3 transformation,

$$q \rightarrow Uq, \quad A_\nu \rightarrow UA_\nu U^{-1} - i/g(\partial_\nu U)U^{-1}, \quad (1)$$

where q is the quark field, A_ν is the gauge field and $U(x, \tau)$ are elements of SU(3) with $U(x, 1/T) = \exp(-2i\pi k/3)U(x, 0)$. This means that $\Omega_{\text{QCD}}(\theta)$ is invariant under the extended \mathbb{Z}_3 transformation [36],

$$\begin{aligned} \theta &\rightarrow \theta + 2\pi k/3, \\ q &\rightarrow Uq, \quad A_\nu \rightarrow UA_\nu U^{-1} - i/g(\partial_\nu U)U^{-1}. \end{aligned} \quad (2)$$

The thermodynamic potential $\Omega_{\text{QCD}}(\theta)$ is transformed into $\Omega_{\text{QCD}}(\theta + 2\pi k/3)$ by the first transformation of Eq. (2) and it is transformed back into $\Omega_{\text{QCD}}(\theta)$ by the \mathbb{Z}_3 transformation, that is, by the second and third equations of Eq. (2). All quantities invariant under the extended \mathbb{Z}_3 transformation, such as the thermodynamic potential and the chiral condensate, keep the RW periodicity. Meanwhile, the Polyakov loop Φ is transformed as $\Phi \rightarrow \Phi e^{-i2\pi k/3}$ under the transformation (2) and then does not have the RW periodicity. However, this problem can be solved by introducing the modified Polyakov loop $\Psi = \Phi e^{i\theta}$ [36] that is invariant under the extended \mathbb{Z}_3 transformation. As an essential property, thus, QCD has the extended \mathbb{Z}_3 symmetry and it is realized as the RW periodicity in the μ_1 region.

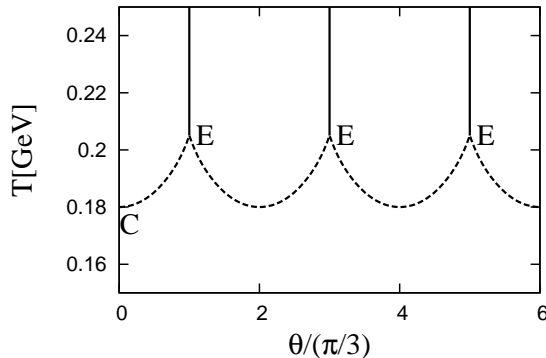


Fig. 1: Phase diagram on the θ - T plane predicted by the PNJL model. This diagram has a periodicity of $\theta = 2\pi/3$. The dashed curves represent crossover deconfinement phase transitions, while the solid lines represent the RW phase transition and its \mathbb{Z}_3 images. Points E are endpoints of the RW phase transitions. Point C is a pseudocritical transition point of the crossover deconfinement phase transition at $\theta = 0$.

Among many effective models proposed so far the PNJL model is only a realistic effective model with both the extended \mathbb{Z}_3 symmetry and chiral symmetry [36, 40, 41]. As a result of this property, the PNJL model succeeds in reproducing the RW periodicity [36, 41]. Figure 1 shows the two-flavor phase diagram in the θ - T plane predicted by the PNJL model; the details of the PNJL calculation will be described in Sec. II. The dashed curves represent crossover deconfinement phase transitions, where the pseudocritical temperature at each θ is determined by the peak position of the Polyakov-loop susceptibility.

Roberge and Weiss also showed by using the perturbative and the strong coupling QCD that $\Omega_{\text{QCD}}(\theta)$ is smooth at $\theta = \pi/3 \pmod{2\pi/3}$ when T is low, but not when T is high [42].

This indicates that there exists a phase transition above a temperature T_E . This discontinuity of $d\Omega_{\text{QCD}}(\theta)/d\theta$ is called the RW phase transition. The RW phase transition is known to be first order at $T > T_E$, but the order at the endpoint $T = T_E$ is not clarified yet. The presence of the first-order RW phase transition is confirmed by LQCD [4–10]. In Fig. 1, the solid line represents the RW phase transition predicted by the PNJL calculation. Point E is the endpoint of the RW phase transition. Obviously, this phase transition also has the RW periodicity. This success of the PNJL model suggests a possibility that the phase diagram in the μ_R region is determined from the thermodynamics in the μ_I region by using the PNJL model, the parameters of which are fitted to reproduce LQCD data in the μ_I region. Actually an analysis along this line has been made very recently in Ref. [41]. Thus, deep understanding of the phase structure in the μ_I region is important to determine the phase diagram in the μ_R region.

The study of the μ_I region has another important aspect. Roberge and Weiss found that at $T > T_E$ three \mathbb{Z}_3 vacua come out alternatively as θ varies from 0 to 2π and showed that at $\theta = \pi/3 \pmod{2\pi/3}$ a transition from one of \mathbb{Z}_3 vacua to another happens [42]. This mechanism is an origin of the RW phase transition appearing at $\theta = \pi/3 \pmod{2\pi/3}$. We call this mechanism the RW mechanism. At $\theta = 0$, one of three vacua is selected. At $T < T_E$, there is no \mathbb{Z}_3 vacua, and hence the RW mechanism does not take place.

In Fig. 1, the dashed curve between points C and E represents a line of crossover deconfinement transition. It is natural to think that the behavior of the crossover deconfinement transition on the line and particularly at point C is influenced by the critical behavior of the RW phase transition at point E. The RW phase transition is studied in Ref. [11] by LQCD with four-flavor staggered fermions. The work suggests that the critical behavior of the RW phase transition at point E is essential to nonperturbative features of strongly coupled quark-gluon plasma (sQGP) appearing at $\mu = 0$ and $T_C < T < 3T_C$, where T_C is a temperature of point C in Fig. 1. Thus, the study on the RW phase transition is also important to understand properties of the crossover deconfinement transition and sQGP at $\mu = 0$.

In this paper, using the two-flavor PNJL model, we investigate properties of the RW mechanism and the RW phase transition as a consequence of the mechanism. Concretely, the following three points are argued. First, we show that in the RW phase transition the charge conjugation (C) symmetry is spontaneously broken, while the extended \mathbb{Z}_3 symmetry

(the RW periodicity) is preserved. Second, we show that the RW phase transition is of second order at the endpoint $(\theta, T) = (\pi/3, T_E)$. In the μ_R region, it is well known that the chiral phase transition is of second order at the critical endpoint [13, 17, 18]. Singular behaviors near the critical endpoints are different between the two second-order phase transitions. Third, we argue that the crossover deconfinement transition at $\mu = 0$ is a remnant of the RW phase transition at the endpoint.

In Sec. II, the PNJL model and the extended \mathbb{Z}_3 symmetry are explained briefly. In Sec. III, the RW phase transition and the RW mechanism are analyzed both analytically and numerically. Section IV gives a summary.

II. PNJL MODEL

A. Model setting

We consider the two-flavor PNJL Lagrangian with $\mu = iT\theta$,

$$\begin{aligned} \mathcal{L} = & \bar{q}(i\gamma_\nu D^\nu - m_0)q \\ & + G_s[(\bar{q}q)^2 + (\bar{q}i\gamma_5\vec{\tau}q)^2] - \mathcal{U}(\Phi[A], \Phi[A]^*, T), \end{aligned} \quad (3)$$

where m_0 is the current quark mass, $D^\nu = \partial^\nu + iA^\nu - i\mu\delta_0^\nu$ and $A^\nu = \delta_0^\nu g A_a^0 \frac{\lambda_a}{2}$ with the gauge field A_a^ν , the Gell-Mann matrix λ_a and the gauge coupling g . In the NJL sector, $\vec{\tau}$ stands for the isospin matrix, and G_s denotes the coupling constant of the scalar-type four-quark interaction. The Polyakov potential \mathcal{U} , defined in Eq. (8), is a function of the Polyakov loop Φ and its Hermitian conjugate Φ^* ,

$$\Phi = \frac{1}{N_c} \text{tr}_c L, \quad \Phi^* = \frac{1}{N_c} \text{tr}_c L^\dagger, \quad (4)$$

with

$$L(\mathbf{x}) = \mathcal{P} \exp \left[i \int_0^\beta d\tau A_4(\mathbf{x}, \tau) \right], \quad (5)$$

where \mathcal{P} is the path ordering, $A_4 = iA_0$ and $N_c = 3$. In the PNJL model, Φ and Φ^* are treated as classical variables. We also denote Φ by $Re^{i\phi}$, where R and ϕ are the absolute value and the phase of Φ , respectively. In the chiral limit ($m_0 = 0$), the Lagrangian density has the exact $SU(2)_L \times SU(2)_R \times U(1)_v \times SU(3)_c$ symmetry.

Using the mean field approximation (MFA), one can obtain the thermodynamic potential per unit volume [23, 27],

$$\begin{aligned} \Omega = & -2N_f \int \frac{d^3\mathbf{p}}{(2\pi)^3} \left[3E(\mathbf{p}) + \frac{1}{\beta} \ln(1+F) \right. \\ & \left. + \frac{1}{\beta} \ln(1+F^*) \right] + G_s \sigma^2 + \mathcal{U} \end{aligned} \quad (6)$$

with

$$F = 3(\Phi + \Phi^* e^{-\beta E(\mathbf{p})+i\theta}) e^{-\beta E(\mathbf{p})+i\theta} + e^{-3\beta E(\mathbf{p})+3i\theta}, \quad (7)$$

where $N_f = 2$, $\sigma = \langle \bar{q}q \rangle$ is the chiral condensate, $\beta = 1/T$ and $E(\mathbf{p}) = \sqrt{\mathbf{p}^2 + M^2}$ with the effective quark mass $M = m_0 - 2G_s \sigma$. We use \mathcal{U} of Refs. [23, 37] that has a strong coupling inspired form,

$$\mathcal{U} = -bT \left[54e^{-a/T} \Phi \Phi^* + \ln(1+G) \right], \quad (8)$$

with

$$G = -6\Phi\Phi^* + 4(\Phi^3 + \Phi^{*3}) - 3(\Phi\Phi^*)^2. \quad (9)$$

The constant parameter a is taken to be 664MeV so as to reproduce the LQCD result on pure gauge that the first-order deconfinement phase transition takes place at $T = T_0 = 270\text{MeV}$ [23, 37].

The vacuum term (the first term of the right-hand side of Eq. (6)) Ω^{vac} diverges. It is then regularized by the three-dimensional momentum cutoff Λ :

$$\int \frac{d^3\mathbf{p}}{(2\pi)^3} \rightarrow \frac{1}{2\pi^2} \int_0^\Lambda dp p^2. \quad (10)$$

Following Ref. [23], we regularize the vacuum part, but not the thermal part. Even if the thermal part is regularized, it does not change the present result much unless T is much larger than T_E .

The parameter b in \mathcal{U} means a mixing strength between the chiral and deconfinement phase transitions, and is chosen to be $0.015\Lambda^3$ to reproduce the two-flavor LQCD data in which a crossover deconfinement transition occurs around $T_C \simeq 180\text{MeV}$; in ref. [37], b is taken to be $0.03\Lambda^3$ to reproduce $T_C \simeq 200\text{MeV}$ in the three-flavor case.

Hence, the present model has three parameters m_0 , Λ , G_s in the NJL sector. Following Ref. [19], we use $m_0 = 5.5 \text{ MeV}$, $\Lambda = 0.6315 \text{ GeV}$, and $G_s = 5.498 \text{ GeV}^{-2}$ that reproduce the pion decay constant $f_\pi = 93.3\text{MeV}$ and the pion mass $M_\pi = 138\text{MeV}$.

In the μ_1 case, Ω and σ are real, while Φ^* is the complex conjugate to Φ [36]. Variables, $X = \Phi, \Phi^*$ and σ , satisfy the stationary conditions,

$$\partial\Omega/\partial X = 0. \quad (11)$$

The thermodynamic potential $\Omega(\theta)$ at each θ is then obtained by inserting the solutions $X(\theta)$ in Eq. (6). The thermodynamic potential $\Omega(\theta)$ thus obtained does not give the global minimum of Ω necessarily. Actually in the case of high T , there exist local minima (unstable solutions) in addition to the global minimum (the stable ground-state solution), as shown later with numerical calculations.

B. Extended \mathbb{Z}_3 symmetry

The thermodynamic potential Ω of Eq. (6) is invariant under the extended \mathbb{Z}_3 transformation,

$$\begin{aligned} e^{\pm i\theta} &\rightarrow e^{\pm i\theta} e^{\pm i2\pi k/3}, \\ \Phi(\theta) &\rightarrow \Phi(\theta) e^{-i2\pi k/3}, \quad \Phi(\theta)^* \rightarrow \Phi(\theta)^* e^{i2\pi k/3}. \end{aligned} \quad (12)$$

This is easily understood by introducing the modified Polyakov loop $\Psi \equiv e^{i\theta}\Phi$ and $\Psi^* \equiv e^{-i\theta}\Phi^*$ invariant under the transformation (12). The extended \mathbb{Z}_3 transformation is then rewritten as

$$e^{\pm i\theta} \rightarrow e^{\pm i\theta} e^{\pm i2\pi k/3}, \quad \Psi(\theta) \rightarrow \Psi(\theta), \quad \Psi(\theta)^* \rightarrow \Psi(\theta)^*, \quad (13)$$

and Ω as

$$\Omega = \Omega^{\text{vac}} + \Omega^{\text{ther}} + \mathcal{U}, \quad (14)$$

with

$$\Omega^{\text{vac}} = -2N_f \int \frac{d^3\mathbf{p}}{(2\pi)^3} 3E(\mathbf{p}) + G_s \sigma^2, \quad (15)$$

$$\Omega^{\text{ther}} = -\frac{2N_f}{\beta} \int \frac{d^3\mathbf{p}}{(2\pi)^3} \left[\ln(1 + F) + \ln(1 + F^*) \right], \quad (16)$$

$$\mathcal{U} = -bT \left[54e^{-a/T} \Psi\Psi^* + \ln(1 + G) \right], \quad (17)$$

where

$$F = 3\Psi e^{-\beta E(\mathbf{p})} + 3\Psi^* e^{-2\beta E(\mathbf{p})} e^{3i\theta} + e^{-3\beta E(\mathbf{p})} e^{3i\theta}, \quad (18)$$

$$G = -6\Psi\Psi^* + 4(\Psi^3 e^{-3i\theta} + \Psi^{*3} e^{3i\theta}) - 3(\Psi\Psi^*)^2. \quad (19)$$

Obviously, Ω is extended \mathbb{Z}_3 invariant, since it is a function of only extended \mathbb{Z}_3 invariant quantities, $e^{3i\theta}$ and $X = \sigma$, Ψ and Ψ^* . The explicit θ dependence appears only through the factor $e^{3i\theta}$ in Eq. (14). Hence, if the solutions $\{X\}$ are uniquely given, they have $X = X(e^{3i\theta})$. Inserting the solutions back into Eq. (14), one can see that $\Omega = \Omega(e^{3i\theta})$. Thus, $\Omega(\theta)$ and $X(\theta)$ have the RW periodicity, $\Omega(\theta) = \Omega(\theta + 2\pi k/3)$ and $X(\theta) = X(\theta + 2\pi k/3)$, because they are extended \mathbb{Z}_3 invariant. However, the situation is more complicated at high T , since three sets of solutions, X_k ($k = 0, \pm 1$), are given; this will be discussed in Sec. III B.

III. ANALYTIC AND NUMERICAL RESULTS

A. RW phase transition

Under the charge conjugation (C), the Polyakov loop and the chemical potential μ are transformed as $\Phi \rightarrow \Phi^*$ and $\mu \rightarrow -\mu$, respectively; for example, see Refs. [24, 43]. This indicates that the modified Polyakov loop $\Psi = \Phi e^{i\theta}$ is also transformed as $\Psi \rightarrow \Psi^*$. As shown in Eqs. (16) and (17), Ω is invariant under the C transformation. In other words, Ω is invariant under the transformation $\theta \rightarrow -\theta$, if Ψ is replaced by Ψ^* . This means that the solutions $X(\theta)$ of the stationary conditions (11) satisfy

$$\Psi(\theta) = \Psi^*(-\theta), \quad \sigma(\theta) = \sigma(-\theta). \quad (20)$$

Equation (20) indicates that the chiral condensate σ , the absolute value $|\Psi|$ and the real part $\text{Re}[\Psi]$ are θ -even, while the phase $\psi = \arg(\Psi) = \phi + \theta$ and the imaginary part $\text{Im}[\Psi]$ are θ -odd. Inserting the solutions $X(\theta)$ into Eq. (14), one can see that $\Omega(\theta)$ is θ -even. Hence, the derivative $d\Omega(\theta)/d\theta$ and the quark number density $n = -d\Omega/d\mu = -d\Omega/d(iT\theta)$ are θ -odd quantities with the RW periodicity. Such θ -odd quantities $O(\theta)$ with the RW periodicity satisfy

$$\lim_{\epsilon \rightarrow +0} O(\theta - \epsilon) = - \lim_{\epsilon \rightarrow +0} O(\theta + \epsilon) \quad (21)$$

at $\theta = \pi/3 \pmod{2\pi/3}$, because $O(\pi/3 - \epsilon) = -O(-\pi/3 + \epsilon) = -O(\pi/3 + \epsilon)$. Thus, $O(\theta)$ is discontinuous when $\lim_{\epsilon \rightarrow +0} O(\theta + \epsilon)$ is finite. This discontinuity is called the RW phase transition, and realized in the high T region, $T > T_E = 205$ MeV, as shown below.

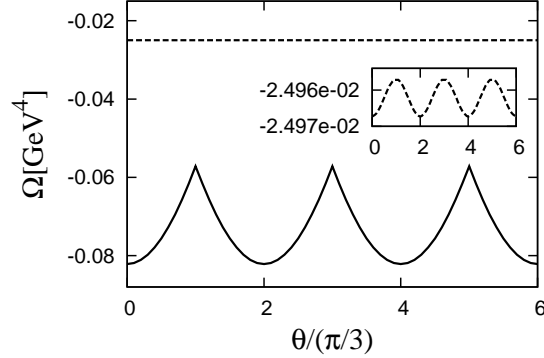


Fig. 2: Thermodynamic potential Ω as a function of θ . The solid curve represents a result of the case of $T = 400$ MeV, and the dashed one corresponds to that of $T = 150$ MeV. The inset represents the θ -dependence of Ω at $T = 150$ MeV in a small scale.

Figure 2 shows θ -dependence of $\Omega(\theta)$ calculated with the PNJL model. At $T = 400$ MeV belonging to the high- T region $T > T_E$, the solid curve has a cusp at $\theta = \pi/3 \pmod{2\pi/3}$. Thus, $d\Omega(\theta)/d\theta$ is discontinuous there. At $T = 150$ MeV belonging to the low- T region $T < T_E$, meanwhile, the dashed curve is smooth everywhere and has the RW periodicity, as shown by the inset. In this low- T case, θ -dependence of Ω is very weak. In the zero- T limit, furthermore, Ω has no θ -dependence, since

$$\Omega|_{T=0} \equiv \lim_{T \rightarrow 0} \Omega = -6N_f \int \frac{d^3\mathbf{p}}{(2\pi)^3} E(\mathbf{p}) + G_s \sigma^2, \quad (22)$$

where σ is obtained by the stationary condition $\partial(\Omega|_{T=0})/\partial\sigma = 0$.

The solution $\Omega(\theta)$ is transformed by the charge conjugation C as $\Omega(\theta) \rightarrow \Omega(-\theta)$. When the solution $\Omega(\theta)$ with θ fixed is considered, C is a symmetry of it only at $\theta = 0$ and π ; note that $\theta = \pi$ is identical with $\theta = -\pi$. The θ -odd quantity $O(\theta)$ such as ψ and n is transformed by C as $O(\pi) \rightarrow -O(-\pi) = -O(\pi)$ and hence not C -invariant at $\theta = \pi$. When $T < T_E$, nevertheless, $O(\theta)$ is a smooth function of θ , so that it is zero at $\theta = \pi$ because of Eq. (21). Thus, we can regard $O(\theta)$ as an order parameter of the C symmetry and then use ψ for this purpose.

Figure 3 shows the T dependence of ψ at $\theta = \pi$. ψ is zero at $T \leq T_E = 205$ MeV, while it is finite at $T > T_E$. Thus, the C symmetry is spontaneously broken above T_E , although

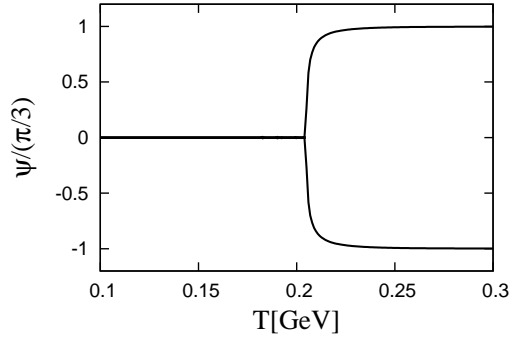


Fig. 3: Phase ψ of the modified Polyakov loop as a function of T in the case of $\theta = \pi$.

it is preserved below T_E . Same phase transition takes place at $\theta = \pi/3$ and $5\pi/3$ as a consequence of the RW periodicity. At $T = T_E$, $d\psi/dT$ is discontinuous, implying that the RW phase transition is of second order there. This result is consistent with the speculation of de Forcrand and Philipsen [4] based on LQCD. Further discussion on this point will be made in subsection III C.

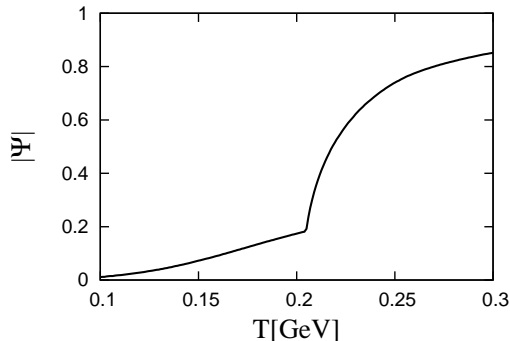


Fig. 4: The absolute value of the modified Polyakov loop as a function of T in the case of $\theta = \pi$.

Figure 4 shows T -dependence of the modulus $|\Psi|$ at $\theta = \pi$. The derivative $d|\Psi|/dT$ is also discontinuous at $T = T_E$. This also implies that the RW phase transition is of second order at the endpoint $(\theta, T) = (\pi/3 \bmod 2\pi/3, T_E)$, although $|\Psi|$ is not zero at $T < T_E$ and then not an exact order parameter of this phase transition.

Figure 5 presents the modulus $|\Psi|$ as a function of T and θ . The second-order phase transition appearing at $\theta = \pi/3$ becomes crossover as θ decreases from $\pi/3$ to 0. Thus, the crossover deconfinement transition at $\theta = 0$, shown by a rapid change of $|\Psi|$ with an increase of T , is a remnant of the second-order RW phase transition at $\theta = \pi/3$.

The PNJL analyses mentioned above are summarized as the phase diagram in Fig. 1.

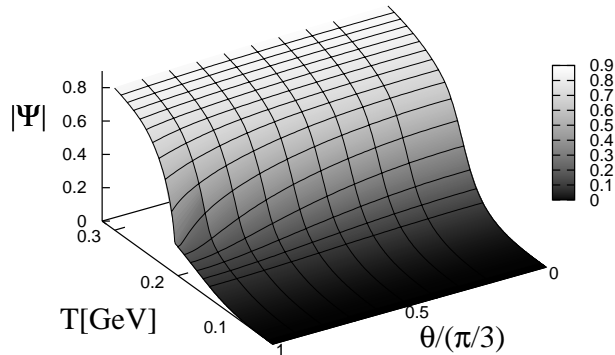


Fig. 5: The absolute value of the modified Polyakov loop as a function of T and θ .

The temperature of point C (the pseudocritical temperature of the deconfinement phase transition at $\theta = 0$) is $T_C = 179$ MeV, and temperature of point E (the endpoint temperature of the RW phase transition) is $T_E = 1.15T_C = 205$ MeV. Thus, T_E is higher than T_C .

B. RW mechanism

We start with the SU(3) pure gauge system. For $\Phi = Re^{i\phi}$, the Polyakov Potential \mathcal{U} is obtained as

$$\mathcal{U} = -bT \left[54e^{-a/T} R^2 + \log(1 - 6R^2 + 8R^3 \cos 3\phi - 3R^4) \right]. \quad (23)$$

The potential \mathcal{U} has a ϕ dependence only through the cubic term $R^3 \cos 3\phi$, that is, the $\Phi^3 + \Phi^{*3}$ term. The fact $-b < 0$ means that \mathcal{U} has a minimum at $\phi = 0 \pmod{2\pi/3}$, if R is not zero. Now we consider the case of $\phi = 0$. Figure 6 show the R dependence of \mathcal{U}/Λ^4 at $\phi = 0$. Three cases of $T/T_0 = 0.99, 1, 1.01$ are shown by solid curves from the top to the bottom, respectively, where $T_0 = 270$ MeV. For each T , \mathcal{U} has two local minima. When $T < T_0$ a global minimum is always located at $R = 0$, but at $T = T_0$ the location jumps from $R = 0$ to 0.45. Thus, a first-order deconfinement transition takes place at $T = T_0$. Due to the $R^3 \cos 3\phi$ term, at $T > T_0$, there are three \mathbb{Z}_3 global minima at $(R, \phi) = (R_0, 0 \pmod{2\pi/3})$, where R_0 is a value between 0.45 and 1. Hence, the ground state of the pure gauge system has a 3-fold degeneracy above T_0 , but no degeneracy below T_0 . In the pure gauge system,

thus, the high- T phase is distinguishable from the low- T one by the number of the vacuum degeneracy.

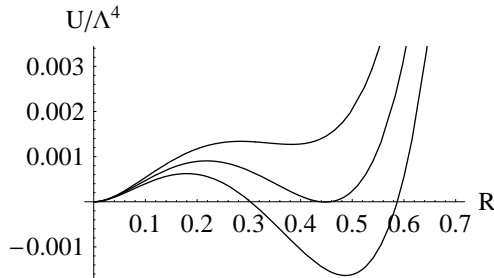


Fig. 6: R dependence of U/Λ^4 at $\phi = 0 \bmod 2\pi/3$. Three solid curves correspond to the cases of $T/T_0 = 0.99, 1, 1.01$, respectively, from the top to the bottom.

Next, we consider the system with dynamical quarks. As a feature of the system, $\Omega(\theta)$ is a smooth function of θ below T_E , as shown in Fig. 2. In order to understand this property, we consider the case of small T . First, we assume that Φ tends to zero and σ does to a finite value σ_0 in the limit of small T . This is a natural assumption and justified below. In the case of small but nonzero T , the stationary conditions (11) for Φ and σ have T dependence through factors $e^{-\beta E(\mathbf{p})}$ and $e^{-\beta a}$. The factor $e^{-\beta E(\mathbf{p})}$ has a maximum $e^{-\beta M}$ at $\mathbf{p} = 0$, and near $T = 0$ the maximum is very close to $\epsilon \equiv e^{-\beta M_0}$ with $M_0 = m_0 - 2G_s \sigma_0$. Hence, the \mathbf{p} integration of $e^{-\beta E(\mathbf{p})}$ is of order ϵ . Further, the factor $e^{-\beta a}$ is of order ϵ^2 because of $a \approx 2M_0$. It is then natural to expand Φ and σ by powers of ϵ : namely, $\Phi = \Phi_1 \epsilon + \Phi_2 \epsilon^2 \dots$ and $\sigma = \sigma_0 + \sigma_1 \epsilon \dots$. One can then derive equations for coefficients Φ_i and σ_i of the ϵ expansion, order by order, from the stationary conditions (11). The equations for the leading-order solutions, σ_0 and Φ_1 , are

$$\sigma_0 = -6N_f \int \frac{d^3\mathbf{p}}{(2\pi)^3} \frac{M_0}{E_0(\mathbf{p})}, \quad (24)$$

$$\Phi_1 = \left\{ \frac{N_f}{b} \int \frac{d^3\mathbf{p}}{(2\pi)^3} e^{-\beta E_0(\mathbf{p}) + \beta M_0} \right\} e^{-i\theta}, \quad (25)$$

where $E_0(\mathbf{p}) = \sqrt{\mathbf{p}^2 + M_0^2}$. Equation (24) does not include T and θ , so that the solution σ_0 is a constant, as expected. In Eq. (25), $\Phi_1 \epsilon$ tends to zero as T decreases, as expected. The absolute value $|\Phi_1|$ does not depend on θ , while the phase of Φ_1 does. Inserting the leading-order solutions into the stationary conditions (11), we can get higher-order solutions;

for example, $\sigma_1 = 0$ and

$$\Phi_2 = \left\{ 2|\Phi_1|^2 + \frac{N_f}{b} \int \frac{d^3\mathbf{p}}{(2\pi)^3} e^{-2\beta E_0(\mathbf{p})+2\beta M_0} \right\} e^{2i\theta}, \quad (26)$$

$$\sigma_2 = \frac{12N_f|\Phi_1|}{C_0} \int \frac{d^3\mathbf{p}}{(2\pi)^3} \frac{M_0}{E_0(\mathbf{p})} e^{-\beta E_0(\mathbf{p})+\beta M_0}, \quad (27)$$

$$\begin{aligned} \sigma_3 &= \frac{12N_f}{C_0} \int \frac{d^3\mathbf{p}}{(2\pi)^3} \frac{M_0}{E_0(\mathbf{p})} \cos(3\theta) \\ &\times \left\{ |\Phi_2| e^{-\beta E_0(\mathbf{p})+\beta M_0} + 2|\Phi_1| e^{-2\beta E_0(\mathbf{p})+2\beta M_0} + e^{-3\beta E_0(\mathbf{p})+3\beta M_0} \right\} \end{aligned} \quad (28)$$

with

$$C_0 \equiv 1 - 12N_f G_s \int \frac{d^3\mathbf{p}}{(2\pi)^3} \frac{\mathbf{p}^2}{(E_0(\mathbf{p}))^3} \sim 0.4, \quad (29)$$

where Φ_3 has not been exhibited, because it does not contribute to Ω up to ϵ^3 , as shown below. The second-order solutions, $|\Phi_2|$ and σ_2 , do not depend on θ , but the phase of Φ_2 and the third-order solution σ_3 do. Thus, unique set of solutions, $\sigma = \sum_{n=0} \sigma_n \epsilon^n$ and $\Phi = \sum_{n=1} \Phi_n \epsilon^n$, is obtained at small T . The thermodynamic potential Ω is given by inserting the set of solutions into Eq. (6). Hence, the potential, $\Omega = \sum_{n=0} \Omega^{(n)} \epsilon^n$, thus obtained is unique and then smooth in θ ; note that $|F| \ll 1$ and $|G| \ll 1$ and then $\log(1+F) \approx F$ and $\log(1+G) \approx G$ have no singularity. The factors F and G can also be expanded into $F = \sum_{n=2} F_n \epsilon^n$ and $G = \sum_{n=2} G_n \epsilon^n$ with

$$F_2 = 3|\Phi_1| e^{-\beta E_0(\mathbf{p})+\beta M_0}, \quad G_2 = -6|\Phi_1|^2, \quad (30)$$

$$F_3 = \left\{ 3|\Phi_2| e^{-\beta E_0(\mathbf{p})+\beta M_0} + 3|\Phi_1| e^{-2\beta E_0(\mathbf{p})+2\beta M_0} + e^{-3\beta E_0(\mathbf{p})+3\beta M_0} \right\} e^{3i\theta}, \quad (31)$$

$$G_3 = -4(3|\Phi_1||\Phi_2| - 2|\Phi_1|^3) \cos(3\theta), \dots \quad (32)$$

Eventually, the $\Omega^{(n)}$ are given as

$$\Omega^{(0)} = G_s \sigma_0^2 - 6N_f \int \frac{d^3\mathbf{p}}{(2\pi)^3} E_0(\mathbf{p}), \quad \Omega^{(1)} = 0, \quad (33)$$

$$\Omega^{(2)} = 2G_s \sigma_0 \sigma_2 + 12G_s N_f \sigma_2 \int \frac{d^3\mathbf{p}}{(2\pi)^3} \frac{M_0}{E_0(\mathbf{p})} - 4N_f T \int \frac{d^3\mathbf{p}}{(2\pi)^3} F_2 - bT G_2, \quad (34)$$

$$\begin{aligned} \Omega^{(3)} &= 2G_s \sigma_0 \sigma_3 + 12G_s N_f \sigma_3 \int \frac{d^3\mathbf{p}}{(2\pi)^3} \frac{M_0}{E_0(\mathbf{p})} - 4N_f T \cos(3\theta) \int \frac{d^3\mathbf{p}}{(2\pi)^3} |F_3| \\ &\quad - bT G_3, \end{aligned} \quad (35)$$

up to order ϵ^3 . Thus, Ω has no θ dependence up to order ϵ^2 , and the θ -dependence appears first at order ϵ^3 through the factor $\cos(3\theta)$. Therefore, Ω is a smooth function of $\cos(3\theta)$ at small T , but the θ dependence is very weak, as explicitly shown in Fig. 2.

Above T_E , Ω has a cusp at $\theta = \pi/3 \pmod{2\pi/3}$, as shown in Fig. 2. To understand the nature of the discontinuity, we consider the case of high T , extend N_f to be a continuous variable and take the small N_f limit. Since Ω^{vac} and Ω^{ther} are proportional to N_f , it can be treated perturbatively. To the zeroth order of N_f , the thermodynamic potential is reduced to that for the pure gauge theory. In this gauge dominant case, the thermodynamic potential has a global minimum at $R = R_0$ satisfying $0.45 < R_0 < 1$, as shown in Fig. 6. Therefore, there exist three unperturbed solutions $\Phi_k \equiv |\Phi_k|e^{i\phi_k} = R_0 e^{i2\pi k/3}$ ($k = 0, \pm 1$), since \mathcal{U} is invariant under the \mathbb{Z}_3 transformation.

Inserting the zeroth solutions $\Phi_k = R_0 e^{i2\pi k/3}$ ($k = 0, \pm 1$) into Ω of Eq. (14), one can get three kinds of thermodynamic potentials $\Omega_k(\theta)$ ($k = 0, \pm 1$). For simplicity, we consider the limit of $R_0 \rightarrow 1$. The thermal fermionic parts $\Omega_k^{\text{ther}}(\theta)$ are

$$\begin{aligned} \Omega_k^{\text{ther}}(\theta, \sigma) \sim & -\frac{6N_f}{\beta} \int \frac{d^3\mathbf{p}}{(2\pi)^3} \left[\ln [1 + e^{-\beta E(\mathbf{p})} e^{i\theta + i2\pi k/3}] \right. \\ & \left. + \ln [1 + e^{-\beta E(\mathbf{p})} e^{-i\theta - i2\pi k/3}] \right], \end{aligned} \quad (36)$$

where $E(\mathbf{p}) = \sqrt{\mathbf{p}^2 + (m_0 - 2G_s\sigma)^2}$. The chiral condensate σ in Eq. (36) is determined by the stationary condition $\partial\Omega/\partial\sigma = 0$:

$$\sigma = -2N_f \int \frac{d^3\mathbf{p}}{(2\pi)^3} \frac{3M}{E(\mathbf{p})} D(\mathbf{p}, T, \theta) \quad (37)$$

with

$$D(\mathbf{p}, T, \theta) = 1 - \frac{1}{e^{\beta E(\mathbf{p})} e^{-i\theta - i2\pi k/3} + 1} - \frac{1}{e^{\beta E(\mathbf{p})} e^{i\theta + i2\pi k/3} + 1}. \quad (38)$$

Equations (37) and (38) show that σ is small at high T , independently of N_f , because the factor $D(\mathbf{p}, T, \theta)$ tends to zero in the limit of high T . In the numerical calculations for $N_f = 2$, Φ_k tends to $e^{i2\pi k/3}$ and σ becomes small as T increases. In this sense the present analysis is consistent with the numerical results.

The solutions $\Omega_k(\theta)$ are smooth, but each solution is periodic only with period 2π . Thus, each of the solutions does not have the RW periodicity. This does not mean that a set of the three solutions does not keep the RW periodicity. In order to understand this clearly, we consider the vanishing quark mass limit of $M = 0$ where the analytic forms of $\Omega_k^{\text{ther}}(\theta)$ are available:

$$\Omega_k^{\text{ther}}(\theta) = \frac{6N_f}{\beta^4 \pi^2} \left[\text{Li}_4(e^{i(\theta - 2\pi k/3)}) + \text{Li}_4(e^{-i(\theta - 2\pi k/3)}) \right], \quad (39)$$

where $\text{Li}_4(z)$ is the polynomial logarithm defined by $\text{Li}_4(z) = \sum_{n=1}^{\infty} z^n/n^4$. As shown in Fig. 7 (a), the three solutions $\Omega_k^{\text{ther}}(\theta)$ are smooth but periodic with period 2π , and $\Omega_{\pm 1}^{\text{ther}}(\theta)$ are obviously \mathbb{Z}_3 images of $\Omega_0^{\text{ther}}(\theta)$. As shown in Fig. 7 (b), if the lowest solution is taken at each θ , the ground state (GS) thus connected, $\Omega_{\text{GS}}^{\text{ther}}(\theta)$, is periodic with period $2\pi/3$ but not smooth at $\theta = \pi/3 \pmod{2\pi/3}$. As a result of this mechanism, $\Omega_{\text{GS}}(\theta) \equiv \Omega^{\text{vac}} + \Omega_{\text{GS}}^{\text{ther}}(\theta) + \mathcal{U}$ is not smooth at $\theta = \pi/3 \pmod{2\pi/3}$, that is, the RW phase transition appears there. We call this mechanism the RW mechanism. In the high T case, thus, the ground state preserves the RW periodicity, i.e. the extended \mathbb{Z}_3 symmetry, although each $\Omega_k^{\text{ther}}(\theta)$ does not. Eventually, the extended \mathbb{Z}_3 symmetry is held at any temperature.

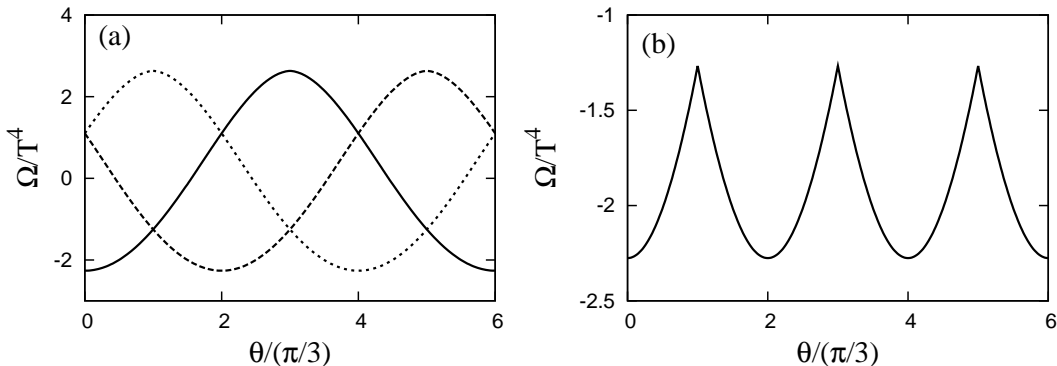


Fig. 7: Perturbative solutions to the thermodynamic potential in its thermal part: (a) the smooth solutions Ω_k^{ther} ($k = 0, \pm 1$) and (b) the ground-state solution $\Omega_{\text{GS}}^{\text{ther}}$. In (a), the solid, the dotted and the dashed curves show the cases of $k = 0$, $k = +1$ and $k = -1$, respectively.

The analyses above based on perturbation are essentially the same as Roberge and Weiss did with perturbative QCD within its one-loop approximation [42, 44]. Actually, the one-loop solutions agree with $\Omega_k^{\text{ther}}(\theta)$ ($k = 0, \pm 1$) of Eq. (39). Thus, at high temperature, the system has three \mathbb{Z}_3 vacua, and they appear alternatively as θ varies from 0 to π . This is the RW mechanism, and when $\theta = 0$ the system belongs to one of the \mathbb{Z}_3 vacua.

The RW mechanism appears also in the full PNJL calculation free from perturbation. However, the situation is more complicated as shown below. The stationary conditions (11) give three sets of solutions, σ_k and $\Phi_k = |\Phi_k|e^{i\phi_k}$ ($k = 0, \pm 1$), as expected. Inserting the solutions into Eq. (14), we have three solutions Ω_k . Figure 8 shows θ -dependence of Ω_k and ϕ_k in the case of $T = 400$ MeV. Surely, there exist three kinds of solutions. At each

θ , however, at least one of the three disappears; the solution Ω_0 vanishes in the region of $0.53\pi < \theta < 1.46\pi$, and the region is shifted by either $2\pi/3$ or $-2\pi/3$ for other solutions. Whenever Ω_k exists, ϕ_k is about $2\pi k/3$ almost independently of θ , while $|\Phi_k|$ depends on θ . The ground state Ω_{GS} is composed of Ω_0 in region (I) $-\pi/3 \leq \theta \leq \pi/3 \pmod{2\pi}$, Ω_{-1} in region (II) $\pi/3 \leq \theta \leq \pi \pmod{2\pi}$, and Ω_1 in region (III) $-\pi \leq \theta \leq -\pi/3 \pmod{2\pi}$.

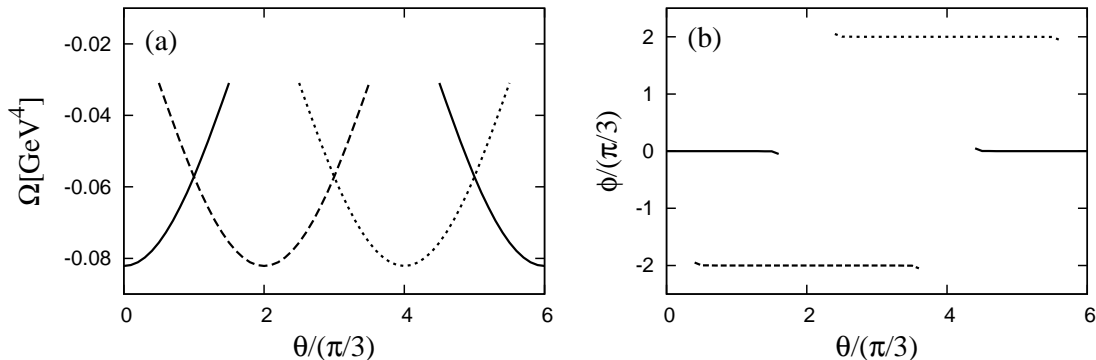


Fig. 8: θ dependence of solutions to the stationary conditions in the case of $T = 400$ MeV: (a) represents Ω_k and (b) does ϕ_k . The solid, the dotted and the dashed curves show the cases of $k = 0$, $k = +1$ and $k = -1$, respectively.

The RW mechanism are analogous to the Dashen phenomenon [45] in the so-called Θ -vacuum. Following Witten's analysis [46] on the Dashen phenomenon, we can discuss the spontaneous breaking of the C symmetry in the RW mechanism. The C transformation changes the sign of θ . Hence, for the thermodynamic potential $\Omega(\theta)$ with θ fixed, C is a symmetry of $\Omega(\theta)$ only at $\theta = 0$ or $\theta = \pi$; note that $\theta = \pi/3 \pmod{2\pi/3}$ has the same property as $\theta = \pi$ because of the RW periodicity. If two of the solutions $\Omega_k(\theta)$ cross each other at $\theta = 0$ and $\theta = \pi$, each solution is C -violating and C interchanges the two solutions there. This Witten's argument on C violation can be explicitly confirmed in this case, as mentioned below. The charge conjugation C transforms the sign of ψ , and hence $\psi = 0$ is invariant under C . In addition, $\psi = \pi$ is also invariant under C because $\psi = \pi$ is identical with $\psi = -\pi$. The solution $\Omega_0(\theta)$ is C -conserving, since it has $\psi = 0$ at $\theta = 0$. Meanwhile, $\Omega_{\pm 1}(\theta)$ are C -violating solutions, because in these solutions ψ is neither 0 nor π at $\theta = \pi$. As shown in Fig. 8(a), the C -violating solutions $\Omega_{\pm 1}(\theta)$ cross each other at $\theta = \pi$, while the C conserving solution $\Omega_0(\theta)$ has no crossing at $\theta = 0$. Thus, the C symmetry is conserved at $\theta = 0$, but spontaneously broken at $\theta = \pi$. This C symmetry breaking appears also at $\theta = \pm\pi/3$ as a consequence of the RW periodicity.

When $T < T_E$, the θ -odd quantity ψ is zero at $\theta = 0$ and π , because ψ is a smooth function of θ satisfying Eq. (21). Hence, the C -symmetry is preserved there. Furthermore, $\psi = 0$ at $\theta = k\pi/3$ with integer k as a result of the RW periodicity. As seen in Sec. III A, θ -dependence of $\Omega(\theta)$ is weak, and then $\psi \sim 0$. Therefore, $\phi = \psi - \theta \sim -\theta$ at low T . On the contrary, when $T > T_E$, ϕ is almost constant in each of regions (I), (II), (III). The $T > T_E$ regime is thus distinguishable from the $T < T_E$ one by the θ -dependence of ϕ (or ψ).

C. Order of RW phase transition at endpoint

Susceptibilities χ_{ij} of σ , $R = |\Psi|$ and $\psi = \arg(\Psi)$ can be written as [23, 32, 35]

$$\chi_{ij} = (K^{-1})_{ij} \quad (i, j = \sigma, R, \psi), \quad (40)$$

where

$$K = \begin{pmatrix} \frac{\partial^2 \Omega}{\partial \sigma^2} & \frac{\partial^2 \Omega}{\partial \sigma \partial R} & \frac{\partial^2 \Omega}{\partial \sigma \partial \psi} \\ \frac{\partial^2 \Omega}{\partial R \partial \sigma} & \frac{\partial^2 \Omega}{\partial R^2} & \frac{\partial^2 \Omega}{\partial R \partial \psi} \\ \frac{\partial^2 \Omega}{\partial \psi \partial \sigma} & \frac{\partial^2 \Omega}{\partial \psi \partial R} & \frac{\partial^2 \Omega}{\partial \psi^2} \end{pmatrix}, \quad (41)$$

is a symmetric matrix of curvatures of Ω and K_{ij} is an (i, j) element of curvature matrix K . Matrix elements $K_{\sigma\psi}$ and $K_{R\psi}$ are θ -odd and then zero at $T \leq T_E$ and $\theta = \pi/3 \pmod{2\pi/3}$, as shown in Eq. (21). Hence, the χ_{ij} is obtained there as

$$\chi_{\psi\psi} = \frac{1}{K_{\psi\psi}}, \quad \chi_{ij} = (K_2^{-1})_{ij} \quad (i, j = \sigma, R), \quad (42)$$

where

$$K_2 = \begin{pmatrix} \frac{\partial^2 \Omega}{\partial \sigma^2} & \frac{\partial^2 \Omega}{\partial \sigma \partial R} \\ \frac{\partial^2 \Omega}{\partial R \partial \sigma} & \frac{\partial^2 \Omega}{\partial R^2} \end{pmatrix}. \quad (43)$$

At the critical point $(\theta, T) = (\pi/3 \pmod{2\pi/3}, T_E)$, thus, the susceptibilities of σ and R decouple from that of ψ , the order parameter of the phase transition.

Figures 9(a) and (b) present T dependence of susceptibilities, $\chi_{\sigma\sigma}$, χ_{RR} and $\chi_{\psi\psi}$, at $\theta = \pi$. The susceptibility $\chi_{\psi\psi}$ has a divergent peak at $T = T_E = 0.2048$ GeV. This indicates that the RW phase transition is of second order at the endpoint $(\theta, T) = (\pi/3 \pmod{2\pi/3}, T_E)$ and also that a θ -odd quantity such as ψ is an order parameter of the phase transition. This result is consistent with the LQCD result [4].

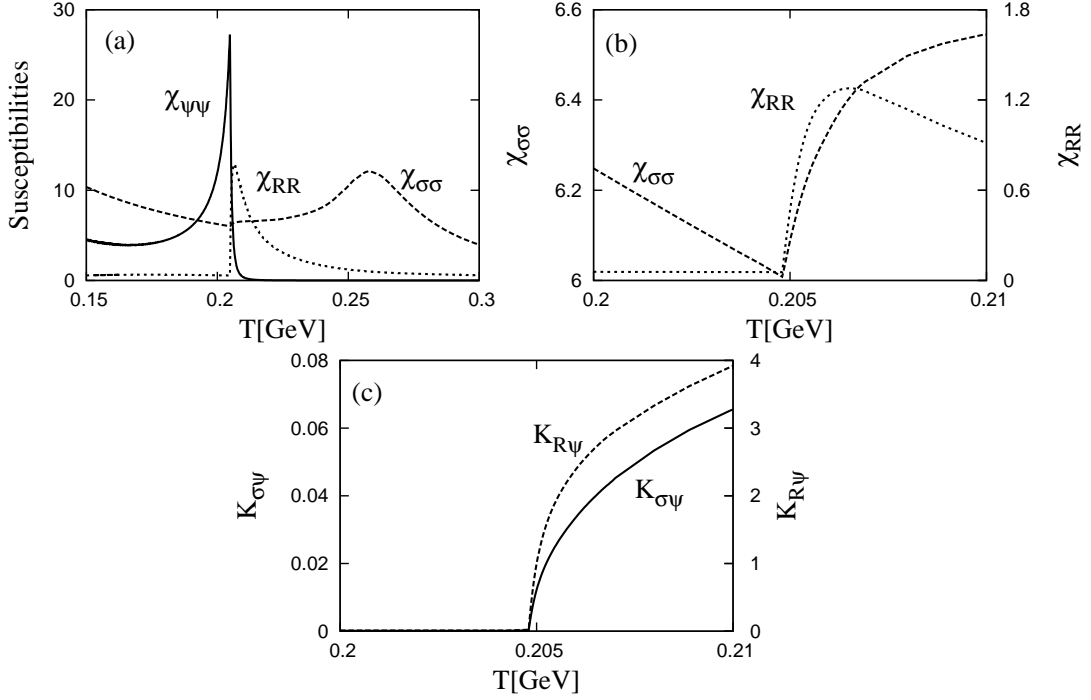


Fig. 9: (a) Susceptibilities of the chiral condensate σ (dashed curve), the absolute value R of the modified Polyakov loop (dotted curve) and the phase of the modified Polyakov loop (solid curve) as a function of T at $\theta = \pi$. $\chi_{\sigma\sigma}$ is divided by T^2 , while χ_{RR} and $\chi_{\psi\psi}$ are multiplied by $10T^4$ and $0.2T^4$, respectively. (b) Susceptibilities of the chiral condensate σ (dashed curve) and the absolute value R of the modified Polyakov loop (dotted curve) near the critical temperature T_E . $\chi_{\sigma\sigma}$ is divided by T^2 , while χ_{RR} and $\chi_{\psi\psi}$ are multiplied by T^4 . (c) Off-diagonal elements $K_{\sigma\psi}$ (solid curve) and $K_{R\psi}$ (dashed curve) are shown as functions of T . $K_{\sigma\psi}$ and $K_{R\psi}$ are divided by T and T^4 , respectively.

As shown in Eq. (42), the divergence comes from the fact that $K_{\psi\psi} = 0$ at the endpoint, and the susceptibilities of the θ -even quantities such as $\chi_{\sigma\sigma}$ and χ_{RR} are irrelevant to $K_{\psi\psi}$. Therefore, the divergent behavior does not affect $\chi_{\sigma\sigma}$ and χ_{RR} . Actually, $\chi_{\sigma\sigma}$ and χ_{RR} have no divergent peak there, as shown in Figs. 9(a) and (b). There is no a priori reason that the transition temperature T_σ defined at the peak position of $\chi_{\sigma\sigma}$ coincides with T_E at $\theta = \pi/3 \pmod{2\pi/3}$. However, it is shown that the vector-type four-quark interaction and the eight-quark interaction make T_σ closer to T_E [41].

This second-order phase transition is accompanied by the spontaneous breaking of charge conjugation (C) symmetry. The C symmetry is a \mathbb{Z}_2 symmetry, since Ω is C -even (θ -even)

and then an even function of C -odd (θ -odd) quantities such as $\text{Im}[\Psi]$ and ψ . Thus, the \mathbb{Z}_2 symmetry is spontaneously broken at $T > T_E$.

In the μ_R region, the second-order chiral phase transition at the critical endpoint is known to be accompanied by a spontaneous \mathbb{Z}_2 symmetry breaking [13]. However, as shown in Refs. [17, 18], the \mathbb{Z}_2 symmetry is not exact such as the C symmetry at the RW endpoint, and the flat direction of the effective potential at the critical endpoint is not the σ direction but a linear combination of the chiral condensate σ , the entropy density s and the quark number density n . Therefore, off-diagonal elements of the curvature matrix K do not vanish, and therefore susceptibilities of σ , s and n diverge simultaneously at the critical endpoint where the determinant of K vanishes.

As seen in Fig. 9(b), $\chi_{\sigma\sigma}$ and χ_{RR} have cusps at T_E . Since $K_{\sigma\psi}$ and $K_{R\psi}$ are θ -odd, as mentioned above, they are zero in the region $T \leq T_E$ where the C symmetry is preserved, but become finite in the region $T > T_E$ where the C symmetry is spontaneously broken via the second-order phase transition. Eventually, as shown in Fig. 9(c), $K_{\sigma\psi}$ and $K_{R\psi}$ have cusps at T_E . This means that in principle all the susceptibilities have cusps at T_E , because they are given by the inverse of the curvature matrix K . However, this singular behavior is masked by the divergence in $\chi_{\psi\psi}$.

The thermodynamic potential Ω of Eq. (12) is a function of variables R , ψ and σ . Taking a minimum of Ω in variation of R and σ with ψ fixed, we can define the potential surface $\Omega(\psi)$ as a function of the order parameter ψ . Figure 10 shows the potential surface at $\theta = \pi$. Panels (a)-(c) show the surface in the cases of $T/T_E = 0.73$, $T/T_E = 1$, 1.05 and $T/T_E = 1.95$, respectively. For the three cases, surely, $\Omega(\psi)$ is \mathbb{Z}_2 symmetric under the transformation $\psi \rightarrow -\psi$. In the case of $T/T_E = 0.73$, there is a minimum at $\psi = 0$. This minimum can be regarded as a ground state Ω_{gr} . The C symmetry is not broken in Ω_{gr} . In the case of $T/T_E = 1.95$, there are two minima at $\psi \approx \pm\pi/3$. These correspond to solutions $\Omega_{\pm 1}$ with $\psi \approx \pm 2\pi/3 + \theta \approx \mp\pi/3 \pmod{2\pi}$ in Fig. 8. It should be noted that there is no minimum at $\psi \sim \pi$. This is consistent with the fact that in Fig. 8 there is no solution with $\phi \sim 0$ at $\theta = \pi$; note that $\phi = \psi - \theta$. At $T = T_E$, the potential surface is flat around $\psi = 0$, indicating that the RW phase transition is of second order at the endpoint $(\theta, T) = (\pi, T_E)$. The same is true also at $\theta = \pi/3 \pmod{2\pi/3}$ as a consequence of the RW periodicity.

Figure 11 presents the potential surface at $\mu = 0$. Panels (a)-(c) correspond to cases of $T/T_E = 0.73$, $T/T_E = 0.87$, 1 and $T/T_E = 1.95$, respectively. Only one solution Ω_0 with

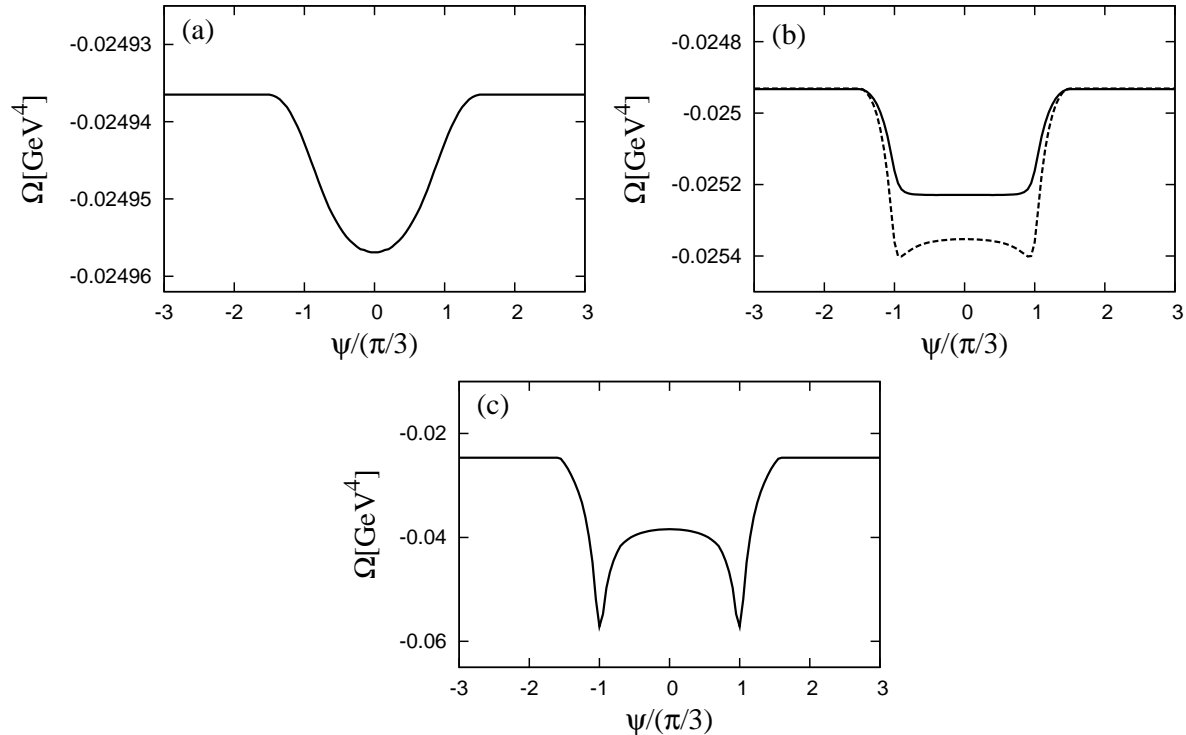


Fig. 10: Potential surface $\Omega(\psi)$ as a function of ψ at $\theta = \pi$: (a) represents the case of $T = 150$ MeV, (b) does two cases of $T = 205$ and 215 MeV and (c) does the case of $T = 400$ MeV. In (b), the case of $T = 205$ MeV (215 MeV) is denoted by the solid (dashed) curve.

$\psi = 0$ appears above T_E , while one solution Ω_{gr} with $\psi = 0$ does below T_E . This is consistent with the fact that in Fig. 8 there is only one solution with $\phi = 0$ at $\theta = 0$. At $\mu = 0$, thus, the phase ψ is always zero for any T . This property guarantees the C conservation, but does not induce any singularity in the T dependence of physical quantities. However, the transition of the ground-state structure from the $T < T_E$ regime to the $T > T_E$ regime makes $|\Psi|$ singular at the endpoint $(\theta, T) = (\pi, T_E)$ of the RW phase transition and then induces a rapid change of $|\Psi|$ even at $\mu = 0$.

IV. SUMMARY

We have analyzed the Roberge-Weiss (RW) mechanism and the RW phase transition, using the PNJL model. Above T_E , three \mathbb{Z}_3 vacua appear alternatively as θ changes from 0 to 2π . As a consequence of this RW mechanism, the extended \mathbb{Z}_3 symmetry (the RW periodicity) is preserved, but C symmetry is broken at $\theta = \pi/3 \bmod 2\pi/3$. This is the

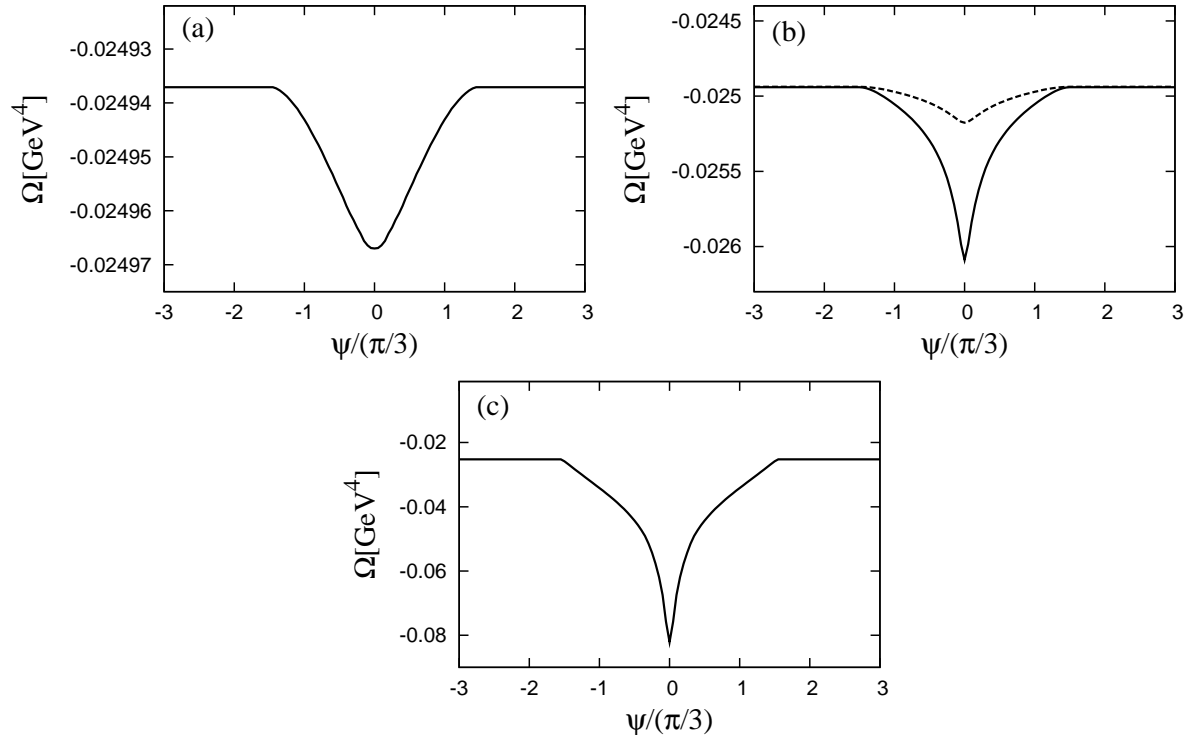


Fig. 11: Potential surface $\Omega(\psi)$ as a function of ψ at $\theta = 0$: (a) represents the case of $T = 150$ MeV, (b) does two cases of $T = 179$ and 205 MeV and (c) does the case of $T = 400$ MeV. In (b) the case of $T = 205$ MeV (179 MeV) is denoted by the solid (dashed) curve .

origin of the RW phase transition. As an order parameter of the phase transition, we can select anyone of θ -odd quantities; a typical one is the phase ψ of the modified Polyakov loop. The RW phase transition is of second order at the endpoint $(\theta, T) = (\pi/3 \bmod 2\pi/3, T_E)$.

The QCD system has \mathbb{Z}_3 vacua above T_E , but does not below T_E . As a consequence of the transition, the Polykov-loop $|\Phi|$ has a singular behavior at the endpoint $(\theta, T) = (\pi/3 \bmod 2\pi/3, T_E)$ of the RW phase transition. The singular behavior induces a rapid change of $|\Phi|$ at $\theta = 0$, as presented in Fig. 5. Thus, the crossover deconfinement transition at $\mu = 0$, defined by the rapid change of $|\Phi|$, is a remnant of the second-order RW phase transition at the endpoint $(\theta, T) = (\pi/3 \bmod 2\pi/3, T_E)$.

Just above T_E , one or two of \mathbb{Z}_3 vacua emerge at each θ in the PNJL model, while all of them appear at each θ in the RW prediction based on perturbation. Thus, the RW mechanism is seen also in the strong-coupling regime which the PNJL model treats, but it is somewhat different from that predicted by Roberge and Weiss in the weak-coupling regime.

Acknowledgments

The authors thank M. Matsuzaki and M. Sato for useful discussions. H.K. also thanks M. Imachi, H. Yoneyama, K. Takenaga and M. Tachibana for useful discussions. This calculation was partially carried out on SX-8 at Research Center for Nuclear physics, Osaka University.

-
- [1] J. B. Kogut and D. K. Sinclair Phys. Rev. D **77**, 114503 (2008).
 - [2] Z. Fodor, and S. D. Katz, Phys. Lett. B **534**, 87 (2002); J. High Energy Phys. **03**, 014 (2002).
 - [3] C. R. Allton, S. Ejiri, S. J. Hands, O. Kaczmarek, F. Karsch, E. Laermann, Ch. Schmidt, and L. Scorzato, Phys. Rev. D **66**, 074507 (2002); S. Ejiri, C. R. Allton, S. J. Hands, O. Kaczmarek, F. Karsch, E. Laermann, and C. Schmidt, Prog. Theor. Phys. Suppl. **153**, 118 (2004).
 - [4] P. de Forcrand and O. Philipsen, Nucl. Phys. **B642**, 290 (2002);
 - [5] P. de Forcrand and O. Philipsen, Nucl. Phys. **B673**, 170 (2003).
 - [6] M. D’Elia and M. P. Lombardo, Phys. Rev. D **67**, 014505 (2003).
 - [7] M. D’Elia and M. P. Lombardo, Phys. Rev. D **70**, 074509 (2004).
 - [8] H. S. Chen and X. Q. Luo, Phys. Rev. **D72**, 034504 (2005); arXiv:hep-lat/0702025 (2007).
 - [9] M. P. Lombardo, arXiv:hep-lat/0612017 (2006).
 - [10] L. K. Wu, X. Q. Luo, and H. S. Chen, Phys. Rev. **D76**, 034505 (2007).
 - [11] M. D’Elia F. Di Renzo and M. P. Lombardo, Phys. Rev. D **76**, 114509 (2007).
 - [12] Y. Nambu and G. Jona-Lasinio, Phys. Rev. **122**, 345 (1961); Phys. Rev. **124**, 246 (1961).
 - [13] M. Asakawa and K. Yazaki, Nucl. Phys. **A504**, 668 (1989).
 - [14] J. Berges and K. Rajagopal, Nucl. Phys. **B538**, 215 (1999).
 - [15] O. Scavenius, Á. Mócsy, I. N. Mishustin, and D. H. Rischke, Phys. Rev. C **64**, 045202 (2001).
 - [16] M. Kitazawa, T. Koide, T. Kunihiro, and Y. Nemoto, Prog. Theor. Phys. **108**, 929 (2002).
 - [17] H. Fujii, Phys. Rev. D **67**, 094018 (2003).
 - [18] H. Fujii, and M. Ohtani, Phys. Rev. D **70**, 014016 (2004).
 - [19] K. Kashiwa, H. Kouno, T. Sakaguchi, M. Matsuzaki, and M. Yahiro, Phys. Lett. B **647**, 446 (2007); K. Kashiwa, M. Matsuzaki, H. Kouno, and M. Yahiro, Phys. Lett. B **657**, 143 (2007).
 - [20] T. Sakaguchi, K. Kashiwa, M. Matsuzaki, H. Kouno, and M. Yahiro, Centr. Eur. J. Phys. **6**,

116 (2008).

- [21] P. N. Meisinger, and M. C. Ogilvie, *Phys. Lett. B* **379**, 163 (1996).
- [22] A. Dumitru, and R. D. Pisarski, *Phys. Rev. D* **66**, 096003 (2002); A. Dumitru, Y. Hatta, J. Lenaghan, K. Orginos, and R. D. Pisarski, *Phys. Rev. D* **70**, 034511 (2004).
- [23] K. Fukushima, *Phys. Lett. B* **591**, 277 (2004).
- [24] A. Dumitru, R. D. Pisarski, and D. Zschiesche, *Phys. Rev. D* **72**, 065008 (2005).
- [25] S. K. Ghosh, T. K. Mukherjee, M. G. Mustafa, and R. Ray, *Phys. Rev. D* **73**, 114007 (2006).
- [26] E. Megías, E. R. Arriola, and L. L. Salcedo, *Phys. Rev. D* **74**, 065005 (2006).
- [27] C. Ratti, M. A. Thaler, and W. Weise, *Phys. Rev. D* **73**, 014019 (2006).
- [28] C. Ratti, S. Rößner, M. A. Thaler, and W. Weise, *Eur. Phys. J. C* **49**, 213 (2007).
- [29] S. Rößner, C. Ratti, and W. Weise, *Phys. Rev. D* **75**, 034007 (2007).
- [30] M. Ciminale, G. Nardulli, M. Ruggieri, and R. Gatto, *Phys. Lett. B* **657**, 64 (2007); M. Ciminale, R. Gatto, N. D. Ippolito, G. Nardulli, and M. Ruggieri, *Phys. Rev. D* **77**, 054023 (2008).
- [31] H. Hansen, W. M. Alberico, A. Beraudo, A. Molinari, M. Nardi, and C. Ratti, *Phys. Rev. D* **75**, 065004 (2007).
- [32] C. Sasaki, B. Friman, and K. Redlich, *Phys. Rev. D* **75**, 074013 (2007).
- [33] B. -J. Schaefer, J. M. Pawłowski, and J. Wambach, *Phys. Rev. D* **76**, 074023 (2007).
- [34] W. J. Fu, Z. Zhang, and Y. X. Liu, *Phys. Rev. D* **77**, 014006 (2008).
- [35] K. Kashiwa, H. Kouno, M. Matsuzaki, and M. Yahiro, *Phys. Lett. B* **662**, 26 (2008).
- [36] Y. Sakai, K. Kashiwa, H. Kouno, and M. Yahiro, *Phys. Rev. D* **77**, 051901(R) (2008); *Phys. Rev. D* **78**, 036001 (2008); Y. Sakai, K. Kashiwa, H. Kouno, M. Matsuzaki, and M. Yahiro, *Phys. Rev. D* **78**, 076007 (2008).
- [37] K. Fukushima, *Phys. Rev. D* **77**, 114028 (2008).
- [38] H. Abuki, M. Ciminale, R. Gatto, G. Nardulli, and M. Ruggieri, *Phys. Rev. D* **77**, 074018 (2008); H. Abuki, M. Ciminale, R. Gatto, N. D. Ippolito, G. Nardulli, and M. Ruggieri, *Phys. Rev. D* **78**, 014002 (2008); H. Abuki, R. Anglani, R. Gatto, G. Nardulli, and M. Ruggieri, *Phys. Rev. D* **78**, 034034 (2008).
- [39] P. Costa, C. A. de Sousa, M. C. Ruivo, and H. Hansen, *arXiv:hep-ph/0801.3616* (2008); P. Costa, M. C. Ruivo, C. A. de Sousa, H. Hansen, and W. M. Alberico, *arXiv:hep-ph/0807.2134* (2008).
- [40] K. Kashiwa, M. Yahiro, H. Kouno, M. Matsuzaki, and Y. Sakai, *J. Phys. G* **36**, 105001 (2009);

- K. Kashiwa, M. Matsuzaki, H. Kouno, Y. Sakai, and M. Yahiro, Phys. Rev. D **79**, 076008 (2009).
- [41] Y. Sakai, K. Kashiwa, H. Kouno, M. Matsuzaki, and M. Yahiro, Phys. Rev. D **79**, 096001 (2009).
- [42] A. Roberge and N. Weiss, Nucl. Phys. **B275**, 734 (1986).
- [43] K. Fukushima and Y. Hidaka, Phys. Rev. D **75**, 036002 (2007).
- [44] N. Weiss, Phys. Rev. D **25**, 2667 (1982).
- [45] R. F. Dashen, Phys. Rev. D **3**, 1879 (1971).
- [46] E. Witten, Ann. Phys. **128**, 363 (1980).